DALTON
FULL PAPER

Complexes of a bis(tetradentate) compartmental pyrazolate ligand: solution studies and solid state structures

Liselotte Siegfried,[a] Thomas A. Kaden,*[a] Franc Meyer,*[b] Peter Kircher[b] and Hans Pritzkow[b]

[a] *Institut für Anorganische Chemie der Universität Basel, Spitalstraße 51, CH-4056 Basel, Switzerland. E-mail: th.kaden@unibas.ch*
[b] *Anorganisch-Chemisches Institut der Universität Heidelberg, Im Neuenheimer Feld 270, D-69120, Heidelberg, Germany. E-mail: franc.meyer@urz.uni-heidelberg.de*

Received 2nd March 2001, Accepted 25th May 2001
First published as an Advance Article on the web 4th July 2001

The stability of Ni^{2+}, Cu^{2+}, and Zn^{2+} complexes with a bis(tetradentate) compartmental pyrazolate ligand (L) was determined in aqueous solution at 25 °C and $I = 0.5$ M (KNO_3). Thereby a series of mononuclear [MLH_n] ($n = 2$, 1, 0, −1, and −2) and dinuclear species [M_2LH_m] ($m = 0, -1, -2$) was observed. The stability of [ML] and [M_2L] increases in the order $Ni^{2+} < Zn^{2+} < Cu^{2+}$, whereby in the case of Ni^{2+} no dinuclear species could be detected. Structural proposals for several species were corroborated by X-ray diffraction studies. In all cases the pyrazolate group has a pronounced tendency to bridge two metal ions.

Introduction

Dinuclear transition metal complexes have received considerable attention over the past several years, mainly due to the increasing interest in cooperative effects between individual metal centers.[1,2] A scaffold for the bimetallic arrangement may be provided by dinucleating ligand matrices that preorganize the two metal ions in suitable proximity.[3] In this regard we have studied a series of pyrazolate-based bimetallic complexes, in which the coordination spheres of the metal ions as well as the accessible range of metal–metal separations can be selectively altered by appropriate changes of chelating substituents attached to the heterocycle.[4–7] The ligand L (Scheme 1) can be

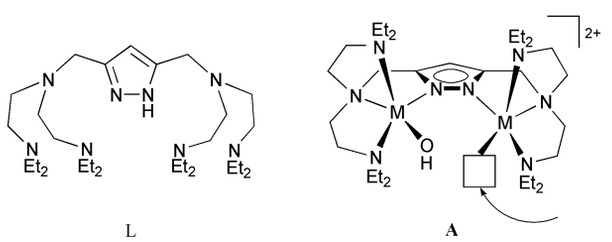

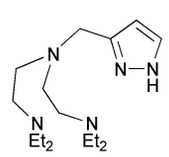

L^a

Scheme 1

viewed as two tren-type coordination groups [tren = tris(2-aminoethyl)amine] coupled by a pyrazole moiety. Owing to the two-atom bridging moiety and the rather short appended ligand side arms, L was shown to enforce metal–metal distances large enough to prevent small ions like hydroxide from occupying a bridging position within the resulting bimetallic pocket.[6] These molecular constraints gave rise to bimetallic type **A** systems (Scheme 1), in which a metal-bound hydroxide is located in close proximity to an accessible coordination site at the adjacent second metal ion – a situation similar to the one encountered in the active sites of various hydrolytic metalloenzymes.[8] In order to use these bimetallic complexes for mimicking functional principles of biological metallohydrolases and to finally understand their observed reactivity, some information about the behavior of complexes of ligand L in aqueous solution is a prerequisite. In the present contribution we report the complexation equilibria and the stability of Ni^{2+}, Cu^{2+} and Zn^{2+} complexes of L in water. Structural proposals for the species in solution are corroborated by solid state X-ray crystallographic results obtained for selected complexes of L and for a related complex of the mononucleating ligand L^a (Scheme 1).[8b]

Table 1 Protonation constants of L at 25 °C and $I = 0.5$ M (KNO_3)

	β_{mlh}	pK_H
LH_4^{4+}	38.08(3)	8.58
LH_3^{3+}	29.46(3)	9.34
LH_2^{2+}	20.15(2)	9.76
LH^+	10.39(3)	10.39

Results and discussion

From potentiometric pH titrations of ligand L the pK_H values were determined (Table 1).We find four relatively high values, which correspond to the protonations of the tertiary amines. Since the differences between the first and second protonation step ($\Delta\log K = 0.63$) as well as that between the third and the fourth ($\Delta\log K = 0.76$) are close to the statistical value of 0.6, and thus indicate that the proton additions are independent of each other, we propose that the sequence of protonation is such that each side of the molecule accepts one proton to give the symmetrical species LH_2^{2+}, followed by third and fourth protons which again are taken up by each side of the molecule to give LH_4^{4+}.

Compared to the ligand carrying two 1,4,7-triazacyclononane units[7] one can note that the first two protonations are lower for L whereas the third and fourth are distinctly higher. This is clearly due to the fact that on one side in L we have tertiary amines, which are less basic than the secondary ones of the ligand with the macrocyclic moieties, and that on the other side the third and fourth proton can be accommodated from the

 DOI: 10.1039/b102015n

Table 2 Complex stability constants of L at 25 °C and $I = 0.5$ M (KNO_3)

Species	Ni^{2+}		Cu^{2+}		Zn^{2+}	
	β_{mlh}	pK_H	β_{mlh}	pK_H	β_{mlh}	pK_H
$[MLH_2]^{4+}$	24.23(3)	8.96	30.80(1)	7.66	25.56(1)	8.07
$[MLH]^{3+}$	15.27(2)	9.27	23.14(4)	9.11	17.49(3)	8.59
$[ML]^{2+}$	6.00(2)	10.31	14.03(6)	10.00	8.90(2)	9.87
$[MLH_{-1}]^{+}$	−4.31(2)		4.03(5)		−0.97(2)	11.31
$[MLH_{-2}]$					−12.28(1)	
$[M_2L]^{4+}$			20.98(3)	5.93	<11.8	
$[M_2LH_{-1}]^{3+}$			15.05(1)	6.68	4.78(3)	7.57
$[M_2LH_{-2}]^{2+}$			8.37(1)		−2.79(1)	

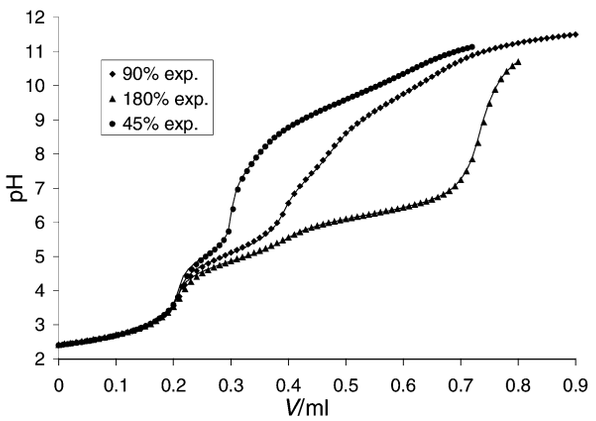

Fig. 1 Titration curves of L in the presence of (●) 0.45, (◆) 0.9 and (▲) 1.8 equivalents of Cu^{2+}.

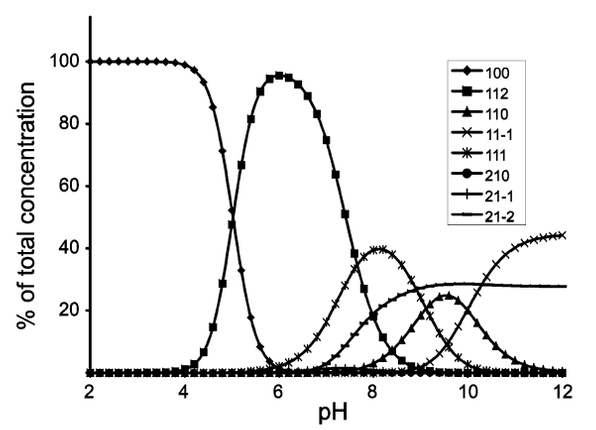

Fig. 2 Species distribution of the complexes of L with 0.45 equivalents of Cu^{2+}. ◆ free metal, ■ MLH_2, * MLH, ▲ ML, × MLH_{-1}, ● M_2L, + M_2LH_{-1}, — M_2LH_{-2}.

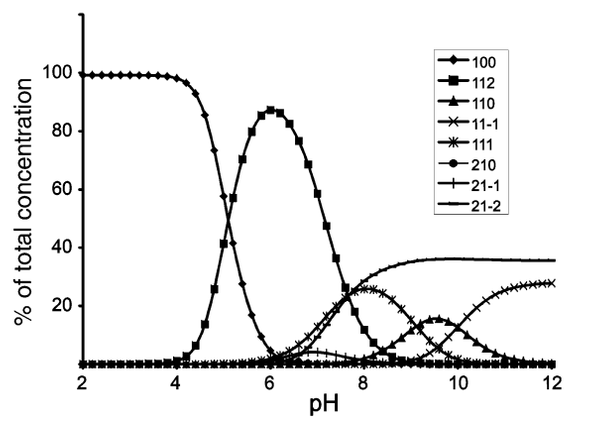

Fig. 3 Species distribution of the complexes of L with 0.9 equivalents of Cu^{2+}. ◆ free metal, ■ MLH_2, * MLH, ▲ ML, × MLH_{-1}, ● M_2L, + M_2LH_{-1}, — M_2LH_{-2}.

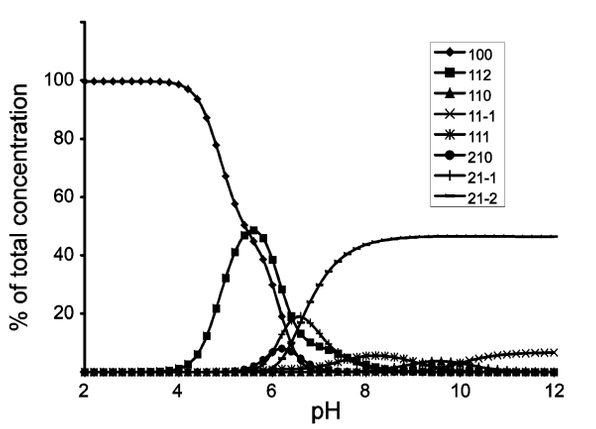

Fig. 4 Species distribution of the complexes of L with 1.8 equivalents of Cu^{2+}. ◆ free metal, ■ MLH_2, * MLH, ▲ ML, × MLH_{-1}, ● M_2L, + M_2LH_{-1}, — M_2LH_{-2}.

electrostatic point of view much better in an open chain system than in a cyclic one.

Titrations of L in the presence of 0.45, 0.9 or 1.8 equivalents of the respective metal ion (M = Ni^{2+}, Cu^{2+} or Zn^{2+}) were analyzed in batch calculations in which all three titration curves are fitted at the same time with one model. The results of the fitting are shown for Cu^{2+} in Fig. 1. This allows the calculation of the stability constants of the mononuclear species $[MLH_2]^{4+}$, $[MLH]^{3+}$, $[ML]^{2+}$, $[MLH_{-1}]^{+}$, and $[MLH_{-2}]$ (the latter only for M = Zn^{2+}) as well as of the dinuclear species $[M_2L]^{4+}$, $[M_2LH_{-1}]^{3+}$, and $[M_2LH_{-2}]^{2+}$. The results are collected in Table 2, and the species distribution diagrams for Cu^{2+} are shown in Fig. 2–4.

Stability constants for all complexes with L are lower than those obtained for the analogous Ni^{2+}, Cu^{2+} and Zn^{2+} complexes of a related pyrazole ligand bearing triazacyclononane (tacn) side arms.[7] This is as expected due to the macrocyclic effect, since 1,4,7-triazacyclononane is ideal for facial binding, and to the presence of secondary instead of tertiary amine groups. The stability of the individual mononuclear $[MLH_n]^{(n+2)+}$ and dinuclear $[M_2LH_m]^{(m+4)+}$ species decreases in the order $Cu^{2+} > Zn^{2+} > Ni^{2+}$.

The observation that a series of protonated 1 : 1 species are found for the mononuclear complexes can be understood if one assumes that the metal ion binds to one side of the ligand, whereas the other side is as in the free ligand *i.e.* either di- or mono-protonated: $[MLH_2]^{4+}$ and $[MLH]^{3+}$. The species $[MLH_{-1}]^{+}$ results either from the deprotonation of the pyrazole group or of a coordinated water molecule and this cannot be determined using potentiometric data alone. Also difficult to assess is the exact sequence of deprotonations starting from $[MLH_2]^{4+}$, specifically, at which pH the pyrazole deprotonation takes place, if at all, in the mononuclear complexes.

To support some structural proposals for the mononuclear complexes deduced from the equilibrium measurements in solution, information on the structures of these complexes in the solid state appeared desirable. Unfortunately, no crystalline

Table 3 Selected atom distances (Å) and bond angles (°) for $[NiL^a(EtCN)_2][\ NiL^a(EtCN)(MeOH)](ClO_4)_8$ [**1**$(ClO_4)_8$]

Ni1–N1	2.033(3)	N1–Ni1–N2a[a]	96.3(1)
Ni1–N2a[a]	2.027(3)	N1–Ni1–N60	169.0(1)
Ni1–N3	2.245(3)	N2a–Ni1–N3[a]	176.4(1)
Ni1–N4	2.219(3)	N4–Ni1–N70	167.3(1)
Ni1–N60	2.102(3)	N101–Ni2–N102b[b]	95.9(1)
Ni1–N70	2.188(3)	N101–Ni2–N160	169.4(1)
Ni2–N101	2.029(3)	N102b–Ni2–N103[b]	177.0(1)
Ni2–N102b[b]	2.043(3)	N104–Ni2–O170	168.0(1)
Ni2–N103	2.233(3)		
Ni2–N104	2.222(3)		
Ni2–N160	2.086(3)		
Ni2–O170	2.168(3)		
N1–N2	1.371(4)		
Ni1 · · · Ni1a[a]	4.039(1)		
N101–N102	1.369(4)		
Ni2 · · · Ni2b[b]	4.060(1)		

[n] Symmetry elements: [a] $1-x, 2-y, 1-z$; [b] $1-x, 2-y, -z$

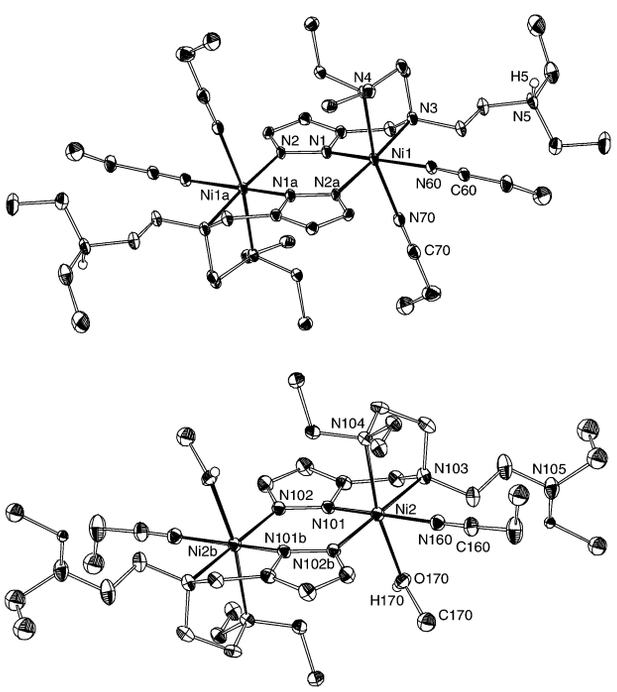

Fig. 5 View of the molecular structure of the two different dinuclear cations of **1** (30% probability ellipsoids). In the interest of clarity all hydrogen atoms have been omitted apart from those bonded to O and N that have been located and refined.

material could be obtained for any species of L with a 1 : 1 metal to ligand ratio. Thus a closely related nickel(II) complex of the mononucleating ligand L^a was prepared independently and its structure determined. The molecular structure of the cation of "$[NiL^a](ClO_4)_2$" in the solid state as revealed by X-ray crystallography is shown in Fig. 5. Selected atom distances and bond angles are listed in Table 3.

The nickel ions are found to be six coordinate with their donor environment consisting of two pyrazolate-N and two aliphatic-N donors of one ligand side arm, and two additional solvent molecules. The unit cell contains two independent bimetallic entities $[NiL^aX_2]_2^{4+}$ (**1**, Scheme 2) that differ in the nature of the solvent coligands X bound to the nickel ions: in one dinuclear cation each nickel is coordinated by two propionitrile solvent molecules in addition to L^a (Fig. 5, top), while in the other dinuclear cation one propionitrile and one methanol is bound to each nickel ion (Fig. 5, bottom). Otherwise, both dimeric cations are very similar. In each case the pyrazole is deprotonated and occupies a bridging position, and the proton is picked up by the remaining ligand side arm tertiary amine functions [the protons bound to O170 of the

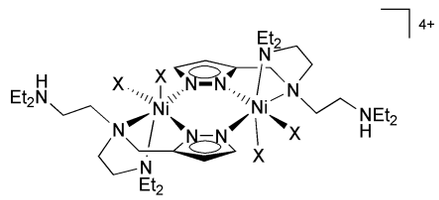

1 (X = EtCN, MeOH)

Scheme 2

MeOH ligand and to N5 could be located in the difference Fourier map; in the crystal lattice, these NH and OH protons are involved in hydrogen bonding to perchlorate counter anions: $d(N5 \cdots O123_{ClO_4}) = 2.75(3)$ Å, $d(O170 \cdots O143_{ClO_4}) = 2.52(3)$ Å].

The structure of **1** underlines the high tendency of the pyrazole heterocycle to adopt a bridging coordination mode in its deprotonated form[9] even if this implies detachment of ligand side arm donor atoms. A bridging binding mode appears to be favored at even lower pH than necessary for deprotonation of the pyrazole-NH if suitable basic functions are available to pick up the excess proton. As a consequence, dimeric structures like **C** or **D** (Scheme 3) might be proposed for the

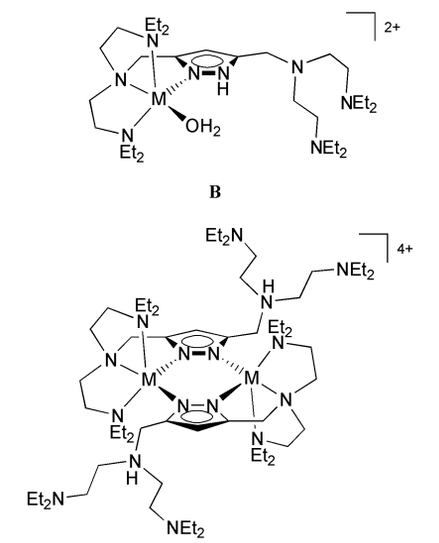

B

C

D

Scheme 3

species $[ML]^{2+}$ as an alternative to the presence of monomeric species **B**. A test for this possibility in modelling our potentiometric measurements, however, does not indicate that dimeric species are present in solution.

The dinuclear complexes found for M = Cu^{2+} and Zn^{2+} begin as $[M_2L]^{4+}$, which deprotonates to $[M_2LH_{-1}]^{3+}$ and $[M_2LH_{-2}]^{2+}$. As can be seen from Fig. 4, $[M_2LH_{-2}]^{2+}$ is the predominant species at pH > 7. In $[M_2L]^{4+}$ one can expect that the two metal ions are bound by the ligand through the amino nitrogens so that no protonation of these is possible. $[M_2L]^{4+}$ is expected to cleave a proton from the pyrazole ring which then can act as a bridging ligand, and from a coordinated water molecule to give a dinuclear hydroxo complex. Here again the exact sequence of

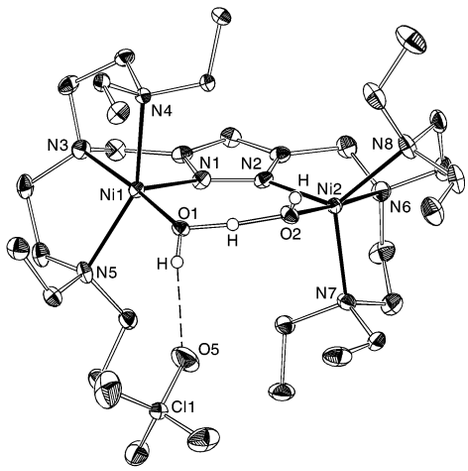

Fig. 6 View of the molecular structure of $[Ni_2(LH_{-1})(H_3O_2)]^{2+}$ (**2**; 30% probability ellipsoids). In the interest of clarity all hydrogen atoms have been omitted apart from those bonded to O.

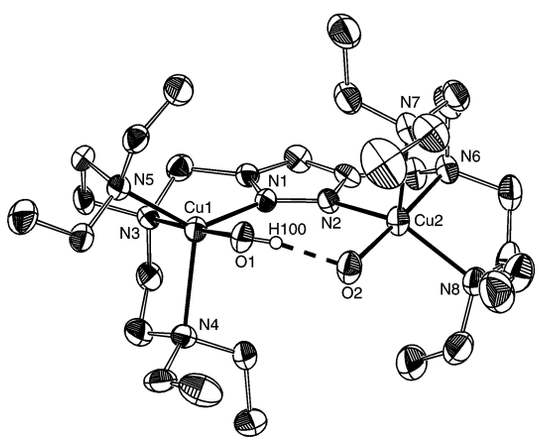

Fig. 7 View of the molecular structure of $[Cu_2(LH_{-1})(H_3O_2)]^{2+}$ (**3**; 30% probability ellipsoids). In the interest of clarity all hydrogen atoms have been omitted apart from the one bonded to O that has been located and refined.

deprotonation cannot be inferred from the potentiometry. Dinuclear species are not observed for $M = Ni^{2+}$ since at higher pH, at which the complexes can form, precipitation of $Ni(OH)_2$ occurs. In view of the use of type **A** compounds as model systems for biological metallohydrolases (see Introduction),[8] the properties of dinuclear species $[M_2LH_{-2}]^{2+}$ and $[M_2LH_{-1}]^{3+}$ in aqueous solution are of prime interest. $[M_2LH_{-2}]^{2+}$ and $[M_2LH_{-1}]^{3+}$ formally stand for complexes **A** and their corresponding acids. From the reaction of L with two equivalents of base and two equivalents of $[Ni(H_2O)_6](ClO_4)_2$ or $[Cu(H_2O)_6](ClO_4)_2$, respectively, complexes **2** and **3** were synthesized on a preparative scale. Both **2** and **3** could be obtained in crystalline form from organic solvents as their ClO_4^- and BPh_4^- salts, respectively, and were analyzed by X-ray crystallography. Molecular structures of the cations $[Ni_2(LH_{-1})(H_3O_2)]^{2+}$ (**2**) and $[Cu_2(LH_{-1})H_3O_2)]^{2+}$ (**3**) are depicted in Fig. 6 and 7, and selected atom distances and bond angles are listed in Tables 4 and 5.

The basic structural features of both cations are identical. As expected from previous results for nickel(II) and zinc(II) complexes of L,[8] each metal ion is found to be five-coordinate within its respective coordination compartment, and a H_3O_2 unit featuring a short intramolecular hydrogen bridge is found within the bimetallic pocket [$d(O1 \cdots O2) = 2.410(3)$ and 2.442(7) Å in **2** and **3**, respectively]. This H_3O_2 bridge can be viewed as a hydrated form of a metal-bound hydroxide ion: a bridging position by the small hydroxide ion itself is prohibited by the large metal–metal separation enforced by the pyrazolate

Table 4 Selected atom distances (Å) and bond angles (°) for $[Ni_2(LH_{-1})(H_3O_2)](ClO_4)_2$ [**2**$(ClO_4)_2$]

Ni1–N1	1.997(3)	N1–Ni1–N3	83.4(1)
Ni1–N3	2.110(3)	N1–Ni1–N4	95.6(1)
Ni1–N4	2.176(2)	N1–Ni1–N5	107.4(1)
Ni1–N5	2.188(3)	N1–Ni1–O1	102.1(1)
Ni1–O1	1.966(2)	N3–Ni1–O1	174.5(1)
Ni2–N2	2.042(3)	N4–Ni1–N5	152.0(1)
Ni2–N6	2.112(3	N2–Ni2–N6	80.2(1)
Ni2–N7	2.141(3)	N2–Ni2–N7	104.3(1)
Ni2–N8	2.211(3)	N2–Ni2–N8	127.5(1)
Ni2–O2	1.965(2)	N2–Ni2–O2	98.1(1)
N1–N2	1.369(4)	N6–Ni2–O2	176.9(1)
Ni1 · · · Ni2	4.380(1)	N7–Ni2–N8	123.2(1)
O1 · · · O2	2.410(3)		
O1 · · · O5	2.936(4)		

Table 5 Selected atom distances (Å) and bond angles (°) for $[Cu_2(LH_{-1})(H_3O_2)](BPh_4)_2$ [**3**$(BPh_4)_2$]

Cu1–N1	2.015(6)	N1–Cu1–N3	82.1(2)
Cu1–N3	2.040(6)	N1–Cu1–N4	104.5(2)
Cu1–N4	2.364(6)	N1–Cu1–N5	136.1(2)
Cu1–N5	2.117(6)	N1–Cu1–O1	95.8(2)
Cu1–O1	1.904(5	N3–Cu1–O1	177.4(2)
Cu2–N2	2.018(5)	N4–Cu1–N5	115.2(2)
Cu2–N7	2.370(7)	N2–Cu2–N7	104.0(2)
Cu2–N6	2.054(6)	N2–Cu2–N6	81.9(2)
Cu2–N8	2.119(7)	N2–Cu2–N8	134.6(3)
Cu2–O2	1.912(5)	N2–Cu2–O2	95.9(2)
N1–N2	1.368(7)	N7–Cu2–O2	97.9(2)
Cu1 · · · Cu2	4.418(2)	N6–Cu2–N8	84.2(2)
O1 · · · O2	2.442(7)	N6–Cu2–O2	177.7(2)

ligand scaffold [$d(Ni \cdots Ni) = 4.380(1)$ Å in **2**, $d(Cu \cdots Cu) = 4.418(2)$ Å in **3**]. In **2**, both the bridging H atom and the two terminal H atoms of the H_3O_2 moiety have been located in the difference Fourier map. The bridging H atom has an almost symmetrical position between the two O atoms [d(O1–H) = 1.18(5) Å, d(O2–H) = 1.23(5) Å], while one of the terminal H atoms forms a hydrogen bridge to a perchlorate counter anion [$d(O1 \cdots O5_{ClO_4}) = 2.936(4)$ Å]. In **3**, only the bridging H atom of the H_3O_2 unit could be located, while the terminal ones presumably form hydrogen bridges to acetone solvent molecules included in the crystal lattice. Based on these crystallographic findings for the solid state, it is suggested that a similar structure exists for the species $[M_2LH_{-2}]^{2+}$ in solution. However, the structure of their corresponding acids, *i.e.* the binding site of the additional proton in $[M_2LH_{-1}]^{3+}$, remains ambiguous. Considering that such systems $[M_2LH_{-1}]^{3+}$ may be regarded as dinuclear coupled versions of two mononuclear tren-type fragments, some indication regarding their structure can be obtained from a comparison of the pK_H values determined for these species with literature values for the hexaaqua ions $[M(H_2O)_6]^{2+}$[10,11] and for the related mononuclear tren-type complexes $[M(tren)(H_2O)_x]^{2+}$ and $[M(Me_6tren)(H_2O)]^{2+}$ ($M = Ni^{2+}$, Cu^{2+}, Zn^{2+}; Table 6).[11–15] Going from the $[M(H_2O)_6]^{2+}$ ions to the five-coordinate $[M(Me_6tren)(H_2O)]^{2+}$ complexes, pK_H values remain quite unchanged, in accordance with a balancing of two contrasting effects, *i.e.* an increase of pK_H due to the exchange of H_2O by N-donors and a decrease of pK_H due to the lower coordination number (in the case of $[M(tren)(H_2O)_x]^{2+}$ the coordination number may be 5 or 6).[16] For $M = Cu^{2+}$ and Zn^{2+}, pK_H values for the deprotonation of metal-bound water in the dinuclear $[M_2LH_{-1}(H_2O)_x]^{3+}$ species are significantly lower (6.68 and 7.57, respectively), confirming the extra stabilization of the formed hydroxide that results from its incorporation into the favorable H_3O_2 intramolecular bridge. Even lower pK_H values (<6) of metal-bound water have been observed upon formation of a hydroxide bridge.[17] It should be noted, however, that these comparisons between the dinuclear species and their mononuclear analogs are hampered by the

Table 6 Comparison of the pK_H values for the hexaaqua ions, for the tren and Me_6tren complexes, and for the dinuclear species $[M_2(LH_{-1})(H_2O)_x]^{3+}$ of Ni^{2+}, Cu^{2+} and Zn^{2+}

Species	$[M(H_2O)_6]^{2+}$[10,11]	$[M(tren)(H_2O)_x]^{2+}$[11–15]	$[M(Me_6tren)(H_2O)]^{2+}$[11–15]	$[M_2(LH_{-1})(H_2O)_x]^{3+}$
Ni^{2+}	9.40 / 10.3	>11 / 12.1	9.53 / 9.6	
Cu^{2+}	7.53 / 7.8	9.37 / 9.4	8.52 / 8.1	6.68
Zn^{2+}	9.60 / 9.5	10.26 / 10.4 / 10.7	9.00 / 8.95 / 8.9	7.57

Table 7 Crystal data and refinement details

	$[NiL^a(EtCN)_2]_2$[$NiL^a(EtCN)$-$(MeOH)]_2(ClO_4)_8$·2MeOH	$[Ni_2(LH_{-1})(H_3O_2)](ClO_4)_2$	$[Cu_2(LH_{-1})(H_3O_2)](BPh_4)_2$·$3COMe_2$
Formula	$C_{84}H_{170}Cl_8N_{26}Ni_4O_{34}$·2MeOH	$C_{29}H_{64}Cl_2N_8Ni_2O_{10}$	$C_{77}H_{104}B_2Cu_2N_8O_2$·$3COMe_2$
M_r	2670.9	873.2	1496.7
Crystal system	Triclinic	Monoclinic	Monoclinic
Space group	$P\bar{1}$	Cc	$P2_1/a$
a/Å	13.017(3)	8.437(1)	17.740(3)
b/Å	13.449(3)	24.095(2)	26.747(5)
c/Å	18.704(4))	19.256(2)	18.024(4)
α/°	97.65(3)	90	90
β/°	106.04(3)	92.828(1)	91.44(2)
γ/°	100.10(3)	90	90
V/Å^3	3041(1)	3910(1)	8550(3)
Z	1	4	4
T/K	200	173	295
μ (Mo-K_α)/mm^{-1}	0.87	1.16	0.56
Unique refl. (R_{int})	11939 (0.031)	8163 (0.026)	8833 (0.063)
Observed refl. $I > 2\sigma(I)$	8935	7655	5396
$R1$	0.056	0.037	0.069
$wR2$ (all data)	0.177	0.097	0.182
Goodness-of-fit	1.041	1.045	1.073

neglect of the additional negative charge provided by the pyrazolate heterocycle, and any structural assumptions deduced from pK_H values and stability constants should thus be viewed with caution.

Experimental

General procedures and methods

All solvents were dried according to established procedures. L and L^a were synthesized according to reported methods.[4,8b] Microanalyses: Mikroanalytische Laboratorien des Organisch-Chemischen Instituts der Universität Heidelberg. IR spectra: Perkin-Elmer 983G. FAB-MS spectra: Finnigan MAT 8230. ESI-MS spectra: Finnigan TSQ 700. UV/Vis spectra: Perkin-Elmer Lambda 19.

Syntheses

Complex 1$(ClO_4)_8$. To a solution of L^a (0.20 g, 0.68 mmol) in propionitrile/methanol (3 : 1; 30 ml) was added $Ni(ClO_4)_2$·$6H_2O$ (0.25 g, 0.68 mmol) and the reaction mixture stirred for 5 h at room temperature. After layering the solution with light petroleum, blue crystals of $[NiL^a(EtCN)_2]_2$ $[NiL^a(EtCN)$-$(MeOH)]_2(ClO_4)_8$, **1**$(ClO_4)_8$ (0.29 g, 0.44 mmol, 65%) gradually formed. MS (FAB$^+$, NOBA): m/z (%) = 805 (30) $[Ni_2L^a{}_2$-$(ClO_4)^+]$, 452 (100) $[NiL^a(ClO_4)^+]$, 352 (85) $[NiL^{a+}]$. IR (KBr pellet) ν_{max} (cm^{-1}) = 3443 (br, m, ν(OH)), 3077 (br, s, ν(NH)), 2981 (w), 2877 (w), 2279 (m, ν(C≡N)), 1471 (m), 1460 (m), 1380 (w), 1259 (w), 1096 (vs, $\nu(ClO_4)$), 794 (m), 623 (s). Found: C, 38.6; H, 6.5; N, 14.3%; Calc. for $C_{84}H_{170}Cl_8N_{26}Ni_4O_{34}$ (1303.4): C, 38.7; H, 6.6; N, 14.0%.

Complex 2$(ClO_4)_2$. A solution of L (0.25 g, 0.48 mmol) in MeOH (30 ml) was treated with KOtBu (0.05 g, 0.48 mmol) and the reaction mixture stirred for 30 min. $Ni(ClO_4)_2$·$6H_2O$ (0.35 g, 0.96 mmol) was then added and stirring continued for 2 h. After evaporation of all volatile material under reduced pressure the residue was taken up in acetone (30 ml) and the solution filtered. Slow diffusion of light petroleum into the solution afforded green crystals of $[Ni_2LH_{-1}(H_3O_2)](ClO_4)_2$, **2**$(ClO_4)_2$ (0.34 g, 0.39 mmol, 81%). MS (FAB$^+$, NOBA): m/z (%) = 771 (100) $[Ni_2(LH_{-1})(H_3O_2)(ClO_4)^+]$, 751 (50) $[Ni_2(LH_{-1})(OH)$-$(ClO_4)^+]$, 672 (35) $[Ni_2(LH_{-1})(H_3O_2)^+]$. IR (KBr pellet) ν_{max} (cm^{-1}) = 3561 (br, s, ν(OH)), 3141 (w), 2968 (s), 2934 (s), 2871 (s), 1524 (w), 1469 (s), 1381 (m), 1312 (m), 1259 (w), 1088 (vs, $\nu(ClO_4)$), 733 (m), 620 (s). Found: C, 40.0; H, 7.4; N, 12.8%; Calc. for $C_{29}H_{64}Cl_2N_8Ni_2O_{10}$ (873.2): C, 39.9; H, 7.4; N, 12.8%.

Complex 3$(BPh_4)_2$. A solution of L (0.25 g, 0.48 mmol) in EtOH (30 ml) was treated with KOtBu (0.05g, 0.48 mmol) and the reaction mixture stirred for 30 min. $Cu(ClO_4)_2$·$6H_2O$ (0.36 g, 0.96 mmol) was then added and stirring continued for 2 h. After addition of $NaBPh_4$ (0.35 g, 1.02 mmol) a light green precipitate immediately formed. This was isolated by filtration and dried under vacuum. Layering a solution of the crude product in acetone with light petroleum gradually afforded green crystals of $[Cu_2LH_{-1}(H_3O_2)](BPh_4)_2$·$3COMe_2$, **3**$(BPh_4)_2$·$3COMe_2$ (1.05 g, 0.35 mmol, 73%). MS (FAB$^+$, NOBA): m/z (%) = 682 (10) $[Cu_2(LH_{-1})(H_3O_2)^+]$, 647 (60) $[(LH_{-1})Cu_2^+]$, 591 (80) $[Cu_2(LH_{-1})(OH)$-$NEt_2^+]$, 370 (100) $[Cu(LH_{-1})$-$N(CH_2$-$CH_2NEt_2)_2^+]$. IR (KBr pellet) ν_{max}(cm^{-1}) = 3605 (br, m, ν(OH)), 3114 (w), 3047 (s), 2975 (s), 2934 (m), 2870 (m), 1937 (w), 1876 (w), 1813 (w), 1700 (s, ν(C=O) acetone), 1574 (m), 1470 (s), 1420 (m), 1378 (m), 1324 (m), 1260 (m), 1180 (m), 1130 (m), 1030 (m), 841 (w), 732 (s), 703 (s), 611 (s), 528 (w). One of the three acetone molecules is removed upon drying the crystals under vacuum. Found: C, 68.9; H, 8.3; N, 7.9%; Calc. for $C_{77}H_{104}$-$B_2Cu_2N_8O_2$·$2COMe_2$ (1438.6): C, 69.3; H, 8.1; N, 7.8%.

Potentiometric titrations

Automatic titrator, as described previously,[18] at 25.0 ± 0.1 °C and I = 0.5 M (KNO_3). Typical concentrations: [L] = 2×10^{-3}

M and $[M^{2+}] = 9 \times 10^{-4}$, 1.8×10^{-3} and 3.6×10^{-3} M, respectively. Titrations were run between pH 2.4 and 11.5. Calibration of the electrode and determination of a_H (0.870) and pK_w (13.85) was performed as described.[18] The evaluation of the protonation and stability constants was done with the program TITFIT,[19] in which the stability constants are defined by eqn. (1) where a_H is the proton activity.

$$\beta_{mlh} = [M_m L_l H_h] / (a_H{}^h [L]^l [M]^m) \quad (1)$$

X-Ray crystallography

The measurements were carried out on a Nonius Kappa CCD diffractometer [complex **1**$(ClO_4)_8$] or a Bruker AXS CCD diffractometer [complex **2**$(ClO_4)_2$] or a Syntex R3 four-circle diffractometer [complex **3**$(BPh_4)_2$] using graphite-monochromated Mo-K_α radiation. For **3**$(BPh_4)_2$ the intensities of three check reflections (measured every 100 reflections) remained constant throughout the data collection (thus indicating crystal and electronic stability) and an absorption correction (ψ scan, $\Delta\psi = 10°$) was applied to the data. Structures were solved by direct methods with the SHELXS-97 and refined with the SHELXL-97 program.[20] Atomic coordinates and thermal parameters of the non-hydrogen atoms were refined in fully or partially anisotropic models by full-matrix least-squares calculation based on F^2. In general the hydrogen atoms were placed at calculated positions and allowed to ride on the atoms they are attached to. In the case of **1**$(ClO_4)_8$ the protons bound to N5 and to O170 could be located in the difference Fourier synthesis and refined. N105 and the ethyl groups bound to it, all ClO_4^- anions, the coordinated methanol and propionitrile as well as the methanol included in the crystal lattice were found disordered. In the case of **2**$(ClO_4)_4$ the protons of the H_3O_2 bridge could be located and refined, while for **3**$(BPh_4)_4$ only H100 was found. The structure determination of **3**$(BPh_4)_4$ was hampered by disorder of the acetone solvent molecules included in the crystal lattice. In Table 7 the data for the structure determinations are compiled.

CCDC reference numbers 160993–160995.

See http://www.rsc.org/suppdata/dt/b1/b102015n/ for crystallographic data in CIF or other electronic format.

Acknowledgements

Funding of this work by the Swiss National Science Foundation (Project No. 20-58958), the Deutsche Forschungsgemeinschaft (Heisenbergstipendium for F. M.) and the Fonds der Chemischen Industrie is gratefully acknowledged. F. M. sincerely thanks Professor Dr G. Huttner for his generous and continuous support.

References

1 (*a*) M. W. Göbel, *Angew. Chem.*, 1994, **106**, 1201; M. W. Göbel, *Angew. Chem., Int. Ed. Engl.*, 1994, **33**, 1141; (*b*) H. Steinhagen and G. Helmchen, *Angew. Chem.*, 1996, **108**, 2489; H. Steinhagen and G. Helmchen, *Angew. Chem., Int. Ed. Engl.*, 1996, **35**, 2339; (*c*) M. Shibasaki, H. Sasai, T. Arai and T. Iida, *Pure Appl. Chem.*, 1998, **70**, 1027; (*d*) D. G. McCollum and B. Bosnich, *Inorg. Chim. Acta*, 1998, **270**, 13; (*e*) E. K. van den Beuken and B. L. Feringa, *Tetrahedron*, 1998, **54**, 12985.

2 (*a*) M. E. Broussard, B. Juma, S. G. Train, W.-J. Peng, S. A. Laneman and G. G. Stanley, *Science*, 1993, **260**, 1784; (*b*) W.-J. Peng, S. G. Train, D. K. Howell, F. R. Fronczek and G. G. Stanley, *Chem. Commun.*, 1996, 2607.

3 See for example: (*a*) S. R. Collinson and D. E. Fenton, *Coord. Chem. Rev.*, 1996, **148**, 19; (*b*) H. Okawa and H. Sakiyama, *Pure Appl. Chem.*, 1995, **67**, 273; (*c*) D. E. Fenton and H. Okawa, *Chem. Ber./Recl.*, 1997, **130**, 433.

4 F. Meyer, S. Beyreuther, K. Heinze and L. Zsolnai, *Chem. Ber./Recl.*, 1997, **130**, 605.

5 M. Konrad, F. Meyer, K. Heinze and L. Zsolnai, *J. Chem. Soc., Dalton Trans.*, 1998, 199.

6 F. Meyer, K. Heinze, B. Nuber and L. Zsolnai, *J. Chem. Soc., Dalton Trans.*, 1998, 207.

7 (*a*) L. Behle, M. Neuburger, M. Zehnder and T. A. Kaden, *Helv. Chim. Acta*, 1995, **78**, 693; (*b*) H. Weller, L. Siegfried, M. Neuburger, M. Zehnder and T. A. Kaden, *Helv. Chim. Acta*, 1997, **80**, 2315; (*c*) H. Weller, T. A. Kaden and G. Hopfgartner, *Polyhedron*, 1998, **17**, 4543.

8 (*a*) F. Meyer and P. Rutsch, *Chem. Commun.*, 1998, 1037; (*b*) F. Meyer, E. Kaifer, P. Kircher, K. Heinze and H. Pritzkow, *Chem. Eur. J.*, 1999, **5**, 1617.

9 Compare also: (*a*) S. Trofimenko, *Prog. Inorg. Chem.*, 1986, **34**, 115; (*b*) G. La Monica and G. A. Ardizzoia, *Prog. Inorg. Chem.*, 1997, **46**, 151.

10 J. E. Huheey, *Anorganische Chemie*, Walter de Gruyter, Berlin/New York, 1988, p. 318.

11 G. Anderegg and V. Gramlich, *Helv. Chim. Acta*, 1994, **77**, 685.

12 J. H. Coates, G. J. Gentle and S. F. Lincoln, *Nature (London)*, 1974, **249**, 773.

13 J. W. Canary, J. Xu, J. M. Castagnetto, D. Rentzeperis and L. A. Marky, *J. Am. Chem. Soc.*, 1995, **117**, 11545.

14 F. Thaler, C. D. Hubbard, F. W. Heinemann, R. van Eldik, S. Schindler, I. Fabian, A. M. Dittler-Klingemann, F. E. Hahn and C. Orvig, *Inorg. Chem.*, 1998, **37**, 4022.

15 M. A. De Rosch and W. C. Trogler, *Inorg. Chem.*, 1990, **29**, 2409.

16 (*a*) R. C. Courtney, R. L. Gustafson, S. Chaberek, Jr. and A. E. Martell, *J. Am. Chem. Soc.*, 1959, **81**, 519; (*b*) R. L. Gustafson and A. E. Martell, *J. Am. Chem. Soc.*, 1959, **81**, 525.

17 See for example: (*a*) C. Wendelstorf, S. Warzeska, E. Kövári and R. Krämer, *J. Chem. Soc., Dalton Trans.*, 1996, 3087; (*b*) L. H. Tan, M. R. Taylor, K. P. Wainwright and P. A. Duckworth, *J. Chem. Soc., Dalton Trans.*, 1993, 2921.

18 H. Gampp, M. Maeder, A. D. Zuberbühler and T. A. Kaden, *Talanta*, 1980, **27**, 573.

19 A. D. Zuberbühler and T. A. Kaden, *Talanta*, 1982, **29**, 201.

20 G. M. Sheldrick, SHELXL-97, Program for Crystal Structure Refinement, Universität Göttingen, 1997; SHELXS-97, Program for Crystal Structure Solution, Universität Göttingen, 1997.